

## Tunable properties of graphene loaded waveguide surrounded by magnetic materials

F. Razzaz<sup>a\*</sup>, A. Nawaz<sup>b</sup>, A. Ghaffar<sup>b</sup>

<sup>a</sup>*Electrical Engineering Department, College of Engineering, Prince Sattam Bin Abdulaziz University, Al-Kharj 16278, Saudi Arabia*

<sup>b</sup>*Department of Physics, University of Agriculture, Faisalabad, Pakistan*

Theoretically analysis has been accomplished for the propagating electromagnetic surface waves (EMSWs) at planar ferrite-graphene-ferrite waveguide structure. The characteristics curves are analyzed for the normalized phase and attenuation phase constant against the operating frequency. The impact of different parameters of ferrite and graphene are observed on the normalize phase and attenuation phase constant. In response to these parameters the structured waveguide exhibits the convenient propagation of electromagnetic surface waves with minimal propagation loss in the terahertz frequency region. The proposed waveguide avails position in nanophotonic devices, terahertz filters, highly integrated terahertz devices and communication systems.

(Received October 13, 2023; Accepted February 9, 2024)

*Keywords:* Surface wave, Plasmonics, Graphene, Waveguide

### 1. Introduction

Electromagnetic surface waves (EMSWs) has attracted much attention in the current arena of nanophotonic field due to their potential applications in imaging, and communication even every aspect of human life. These EMSWs excites at the interface of two dissimilar media and die down exponentially as its moves aside from the interface [1]. Surface Plasmon polaritrons (SPPs) are special kind of EMSWs that propagate at the interface between metal and dielectric. The SPPs has increased curiosity for researchers due to their some extraordinary electromagnetic traits [2, 3]. The conventional photonic devices suffer difficulties in downsizing to nanometer range due to diffraction limit. The surface Plasmon polaritrons overcome this issue making it suitable for the future photonic devices [4]. Furthermore, SPPs also offers potential approach for controlling and manipulating light dispersion and propagation at nanometer range according to desired applications. Currently metal based plasmonic devices are used in society. Metal shows propagation losses at THz frequency band. To overcome this issue graphene material has been introduced. Graphene is one atom thick, flat sheet of carbon atoms, packed in crystalline hexagonal structure. It's attracted considerable attention in photonic, electronic, magnetic, thermal and mechanical properties owing to its unique optical properties, such as large optical absorption, relative high nonlinearity and self-polarization effect [5-8]. The single graphene layer possesses larger thermal conductivity in comparison to other materials, large surface area, zero band structure and high mechanical strength. Recently Literature work showed that by chemical doping or biasing, the graphene can exhibits the metallic properties in the mid-infrared region [9]. Graphene plasmons possess much stronger confinement than the metals with the minimal propagation losses. Graphene can maintain highly cramped Surface Plasmons at terahertz (THz) frequency, enabling the different strategy for guiding THz waves at deep wavelength scale. The characteristics of graphene can potentially be adjusted across higher frequency by altering its doping level and an external gate voltage [10].

Ferrites are anisotropic materials have the lowest magnetic field strength of any permanent magnetic materials with the larger energy product ranging from 0.8 to 5.3 MOe. They retain their performance even at higher temperatures and show best performance with minimal loss of energy.

---

\* Corresponding author: f.kasim@psau.edu.sa  
<https://doi.org/10.15251/DJNB.2024.191.283>

Ferrite cores are the main components that are used in electromagnets, inductors and in transformers where their high electrical resistance leads to very small eddy current losses. Owing to these properties ferrites are essential components for the radar absorbing materials and largely implanted in the design and fabrication of antenna, isolators, circulators and phase shifters [11]. Even with the complexity of shifting DC magnetic bias, due to anisotropic magnetic properties the ferrite-based structures are most preferable choice for the designing the modern reforms antenna. By varying the magnetic bias, the magnetic tensor of ferrite is tailored and used to design the reconfigurable electromagnetic appliances [12-14].

Seyed Ehsan presented an analytical approach to study THz graphene-metal waveguide structure. The simulation results showed that the properties of proposed antenna can be tuned by graphene's chemical potential. The terahertz antenna has potential application in the terahertz devices such as wireless communication in chip and sensing appliances [15]. Gennady Shkerdin demonstrated the characteristics curves for the slab metal waveguide. Transverse electric mode was analyzed against the buffer layer thickness and Fermi energy of graphene. It was concluded that the modes of the composed structured can be tuned by the changing the Fermi energy level near the region of waveguide mode [16]. Bofeng Zhu *et al* demonstrated the graphene surrounded by dielectric tunable infrared waveguide. The proposed structured showed the hyperbolic dispersion characteristics from mid-infrared to far-infrared region and the optical properties of the waveguide were tune by the biasing voltage on the graphene layers [17]. Christopher K proposed the anti-symmetrically isolator waveguide filled with based ferrite material. The theoretical investigation revealed that proposed structures support the band limited unidirectional magneto-static surface wave mode. [18].

Yuliya S. Dadoenkova demonstrated the interaction of surface Plasmon polaritrons of far-infrared region in the structure, semiconductor-graphene-dielectric. The results showed that when phase velocity of surface Plasmon polaritrons matched to drift velocity of charge carrier than the surface waves in the graphene structured were enhanced by drift current in graphene [19]. This work has potential applications in the terahertz region including remote sensing, material characterizing, medical and biological imaging. Due to excess of additional degree of freedom in graphene, this work based on the plasmonic theory open a new gate way for designing the photonic devices in nanometer scale. The proposed structure was investigated analytically and the results obtained can be promising for developing the nonreciprocal components [20].

The electromagnetic surface waves at the interface of graphene surrounded by other dielectric or magnetic, and metal materials are under the consideration for many researchers owing to the easily light confinement for the dielectric waveguides [21-23]. In this paper, the theoretical analysis for the propagation of EMSWs at the interface between graphene surrounded by ferrite media is presented in the terahertz frequency region. Maxwell equations and the boundary conditions are applied to address this complication, the effect of various factors; relaxation time, chemical potential, ferrite permittivity, applied magnetic field, saturation magnetization and the number of graphene layers are studied successfully. The characteristics curves are plotted for the normalized phase, attenuation phase as a function of angular frequency in the THz frequency.

## 2. Formulation and methodology

In this section, methodology of planar structure of ferrite-graphene-ferrite has been discussed. Consider EM surface waves propagate along z-axis and attenuate along x-axis as shown in figure 1.

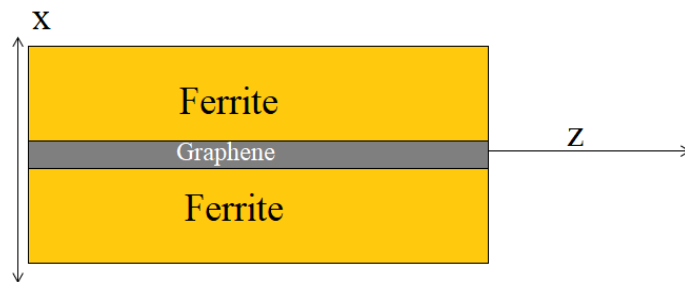


Fig. 1. Geometry of three-layer ferrite-graphene-ferrite waveguide.

The geometry of the model and the width of all the layers are taken in micrometer range. The conductivity of graphene is defined by two portion; intra-bands and inter-bands, therefore it is evaluated from the well-known Kubo's formula [24].

$$\sigma_{intra} = j \frac{TK_B e^2}{\pi \hbar^2 (\omega + \frac{j}{\tau})} \left( \frac{\mu_c}{K_B T} + \text{Log} \left[ 10, \text{Exp} \left( -\frac{\mu_c}{K_B T} + 1 \right) \right] \right) \quad (1)$$

$$\sigma_{inter} = j \frac{e^2}{\pi \hbar} \text{Log} \left[ 10, \frac{2 \text{Abs}[\mu_c] - \hbar \left( \omega + \frac{j}{\tau} \right)}{2 \text{Abs}[\mu_c] + \hbar \left( \omega + \frac{j}{\tau} \right)} \right] \quad (2)$$

$$\sigma_g = \sigma_{intra} + \sigma_{inter} \quad (3)$$

$$\sigma_g = j \frac{TK_B e^2}{\pi \hbar^2 (\omega + \frac{j}{\tau})} \left( \frac{\mu_c}{K_B T} + \text{Log} \left[ 10, \text{Exp} \left( -\frac{\mu_c}{K_B T} + 1 \right) \right] \right) + j \frac{e^2}{\pi \hbar} \text{Log} \left[ 10, \frac{2 \text{Abs}[\mu_c] - \hbar \left( \omega + \frac{j}{\tau} \right)}{2 \text{Abs}[\mu_c] + \hbar \left( \omega + \frac{j}{\tau} \right)} \right] \quad (4)$$

where  $\mu_c$  is the chemical potential taken in eV,  $\tau$  is the relaxation time,  $T$  is temperature,  $e$  is the electron charge,  $K_B$  is the Boltzmann's and  $\hbar$  is the reduced Plank's constant, and  $\omega$  is the operating frequency.

The permeability of ferrite medium is described by the Polder tensor literature in [25].

$$\mu_F = \begin{pmatrix} \mu_a & 0 & i\mu_b \\ 0 & \mu_c & 0 \\ -i\mu_b & 0 & \mu_a \end{pmatrix}, \quad (5)$$

$$\mu_a = \left( 1 + \frac{\omega_0 \omega_m}{\omega_0^2 - \omega^2} \right) \mu_B, \quad \mu_b = \left( \frac{\omega \omega_0}{\omega_0^2 - \omega^2} \right) \mu_B, \quad \mu_c = \mu_B, \quad \mu_B = 1 \quad (6)$$

where  $\omega_0 = \mu_0 \gamma H_0$ ,  $\omega_m = \mu_0 \gamma M_s$ , and here  $\mu_B$  is optical background polder permeability. The  $M_s$  and  $H_0$  is the magnetization and uniform intensity after applying magnetic field  $B_0$ . In this way ferrite-graphene-ferrite waveguide is presented.

The 2-D structure is selected for the presented study, under the physics section in Comsol the "Electromagnetic wave frequency domain" (*ewfd*) is chosen placed in the tree of wave optics. This physics simulates the electromagnetic field distribution at the interface of structured waveguide and solves the electromagnetic wave propagation manipulated by Maxwell's wave equation [26].

$$\nabla \times \mu_r^{-1} \times (\nabla \times E) - k_o^2 \left( \varepsilon_r - \frac{j\sigma}{\omega \varepsilon_o} \right) E = 0 \quad (7)$$

where  $\varepsilon_r$ ,  $\mu_r$ ,  $k_o$ , and  $\sigma$  are the relative permittivity, relative permeability, wavenumber in free space and the conductivity.

Ports are selected to be numeric for different boundaries of proposed model Parametric sweep is applied for the different parameters along with operating frequency to address this

challenge. Then, the file is computed in the terahertz frequency. The normalized phase constant  $Re\left(\frac{\beta}{k_0}\right)$  and propagation loss i.e.,  $Im\left(\frac{\beta}{k_0}\right)$  are plotted against the angular frequency for the various values of chemical potential, relaxation time, number of graphene layers and dielectric constant of ferrite are discussed in detail in next section.

### 3. Results and discussion

The simulated results are presented to explore the study of characteristics of EMSWs in ferrite-graphene-ferrite waveguide structure. Normalized phase constant, attenuation phase constant or propagation loss as the function of angular frequency in THz range under the different values of chemical potential, relaxation time, number of graphene layers, dielectric constant of ferrite film, D.C magnetic field and saturation magnetization are analyzed. Since graphene has extra degree of freedom compared to other plasmonic material. Its conductivity can be easily tuned through chemical potential and relaxation time. The chemical potential of graphene  $\mu_c = \hbar V_f \sqrt{n_c \pi}$  depends on the biasing voltage and the carrier concentration. Figure 2 presents the influence of chemical potential on the normalized phase constant  $Re\left(\frac{\beta}{k_0}\right)$  against angular frequency. The chemical potential extends from  $\mu_c = 0.1$  eV to  $\mu_c = 0.3$  eV and angular frequency 1 to 3 THz. As a result of the increase in chemical potential, the normalized propagation constantly increases. The increase in chemical potential provides the necessary energy for the signal or wave to propagate more efficiently, resulting in a higher normalized propagation constant. It should be mentioned that graphene conductivity is proportional to its chemical potential, making increment in chemical potential the graphene conductivity increases and the propagation loss decreases. Moreover, it is cleared from the plot that increase in  $\mu_c$  the will shift the curves toward higher frequency, similarly down fall in  $\mu_c$  will allow the curves backward toward the lower frequency region, literature in [27, 28]. As cleared from the plot that for  $\mu_c = 0.3$  eV has larger propagation than the  $\mu_c = 0.1$  eV. The presented tunability curves indicate that the EMSWs can be engineered by changing the chemical potential of graphene. Figure 3 illustrates the impact of  $\mu_c$  on attenuation phase constant  $Im\left(\frac{\beta}{k_0}\right)$  or propagation loss against the angular frequency. The variation is presented under different values of chemical potential such as, i.e.,  $\mu_c = 0.1$  eV,  $\mu_c = 0.2$  eV, and  $\mu_c = 0.3$  eV. The increase in chemical potential tends to result in a decrease in propagation loss and peaks are shifted towards low frequency region. The graphical picture evidences that when the angular frequency ranges from 1 to 3 THz, the  $Re\left(\frac{\beta}{k_0}\right)$  linearly increase, literature in [29].

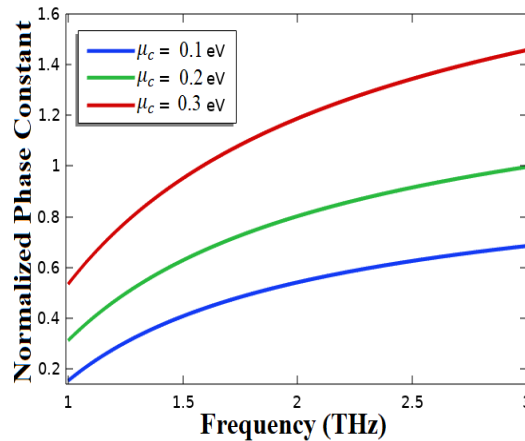


Fig. 2. Influence of " $\mu_c$ " on the normalized propagation constant for ferrite-graphene-ferrite structure.

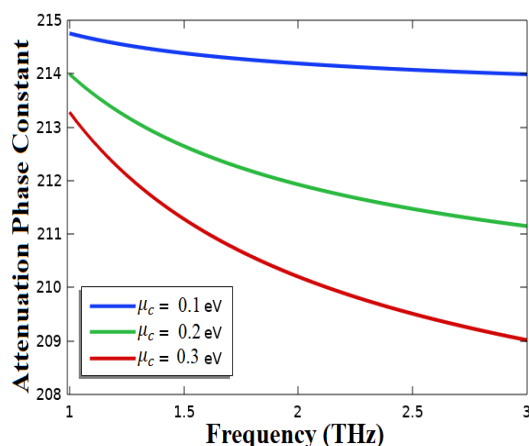


Fig. 3. Influence of " $\mu_c$ " on the propagation loss for ferrite-graphene-ferrite structure.

The influence of relaxation time on Normalized phase constant as the function of angular frequency is also studied. Figure 4 shows the effect of relaxation time on the normalized phase constant  $Re\left(\frac{\beta}{k_0}\right)$  for ferrite-graphene-ferrite interface versus angular frequency. Frequency ranges from 1 to 3 THz while relaxation time increases from  $\tau = 1 \times 10^{-13}$  s to  $\tau = 3 \times 10^{-13}$  s indicated by the blue, green, and red respectively. It is cleared from the plot that as the values of  $\tau$  increases the propagation band gap decreases and the curves shift toward higher frequency, which depicts that the higher confinement of surface waves at the lower values of  $\tau$ . The higher the normalized propagation constant, the shorter the relaxation time, and vice versa. The Figure 5 illustrates the influence of relaxation time on the attenuation phase constant  $Im\left(\frac{\beta}{k_0}\right)$  for the proposed waveguide structure. The variation in peaks indicates that propagation loss can be controlled by relaxation time. Figure 6 and 7 shows the normalized phase constant  $Re\left(\frac{\beta}{k_0}\right)$  and attenuation phase constant  $Im\left(\frac{\beta}{k_0}\right)$  respectively, against the angular frequency for the variable dielectric constant of ferrite film in the THz frequency band. The dielectric constant of ferrite increased from  $\epsilon_f = 8$  to  $\epsilon_f = 14$ . The curves show that the dielectric constant of the ferrite film has significant control on the propagation and modulation for the proposed waveguide structure. As dielectric constant of ferrite film is increased the normalized propagation constant is increases while attenuation decreased. Figure 8 and 9 show the impact of magnetic field on normalized phase constant  $Re\left(\frac{\beta}{k_0}\right)$  and attenuation phase constant  $Im\left(\frac{\beta}{k_0}\right)$  respectively, against angular frequency.

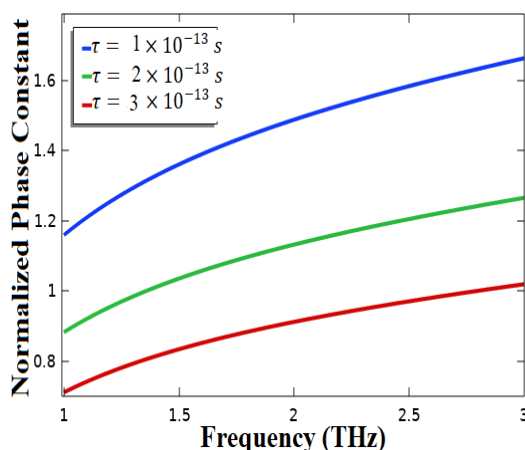


Fig. 4. Impact of " $\tau$ " on the normalized phase constant for ferrite-graphene-ferrite waveguide.

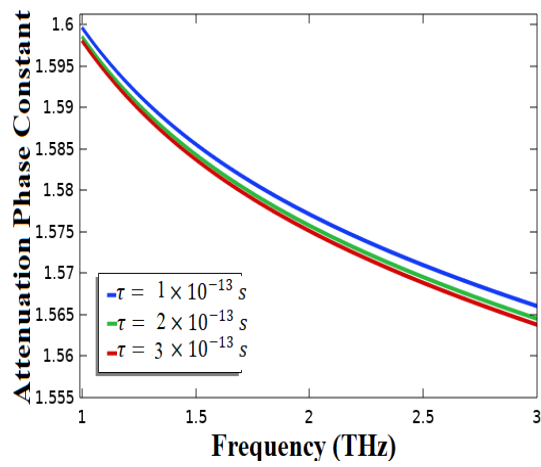


Fig. 5. Impact of " $\tau$ " on attenuation phase constant for ferrite-graphene-ferrite waveguide.

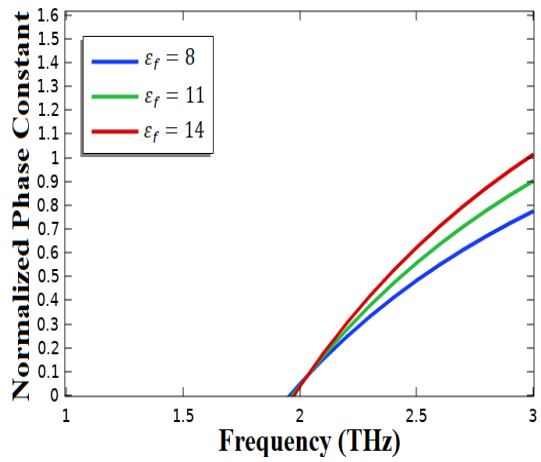


Fig. 6. Effect of dielectric constant of ferrite on the normalized phase for ferrite-graphene-ferrite waveguide structure.

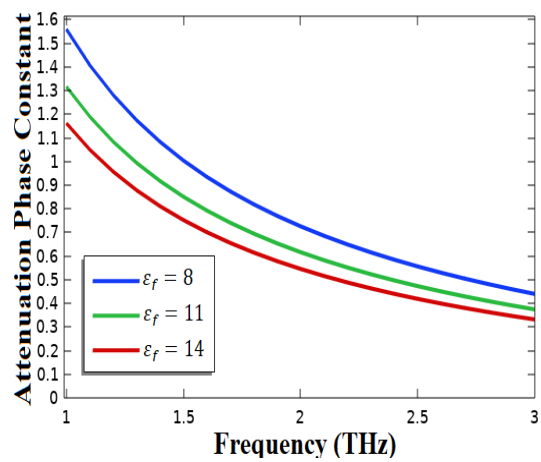


Fig. 7. Effect of dielectric constant of ferrite on the attenuation phase constant for ferrite-graphene-ferrite waveguide.

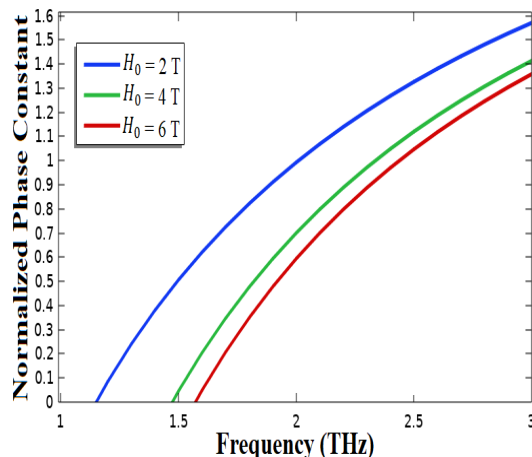


Fig. 8. Effect of magnetic field on the normalized phase against frequency in ferrite-graphene-ferrite waveguide.

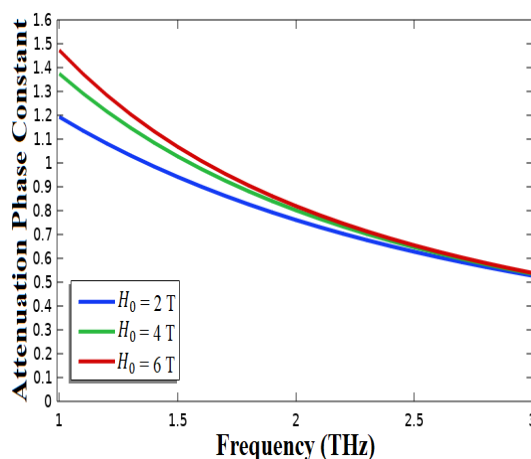


Fig. 9. Effect of magnetic field on the attenuation phase verses frequency in ferrite-graphene-ferrite.

The presence of a magnetic field can significantly influence the behavior of electromagnetic waves propagating through a medium. When a magnetic field is applied perpendicular to wave propagation direction, it induces changes in the normalized propagation constant. It is cleared from the red, blue, and green peaks that increasing magnetic field leads to decrease in bandgap and the curves are moving toward higher frequency with smaller propagation. In contrast the propagation loss is smaller at the lower value that insures the dependence attenuation phase constant on the magnetic behavior of ferrite's magnetic field.

Figure 10 and 11 illustrate the influence of saturation magnetization on normalized phase constant  $Re\left(\frac{\beta}{k_0}\right)$  and attenuation phase constant  $Im\left(\frac{\beta}{k_0}\right)$  respectively, plotted against angular frequency for the structured waveguide. The values taken for the plots are,  $M_S = 500 G$ ,  $M_S = 1500 G$ , and  $M_S = 2500 G$ .

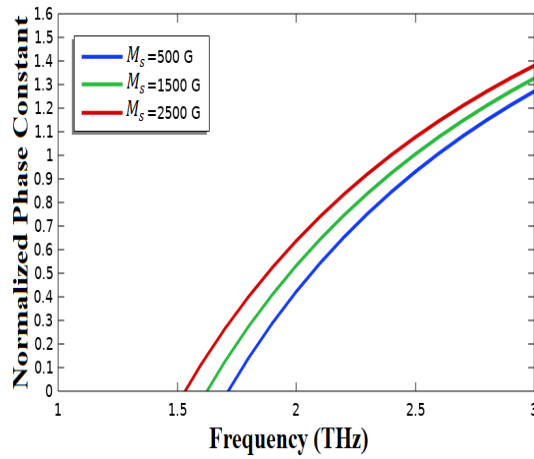


Fig. 10. Influence of saturation magnetization on the normalization for ferrite-graphene-ferrite waveguide.

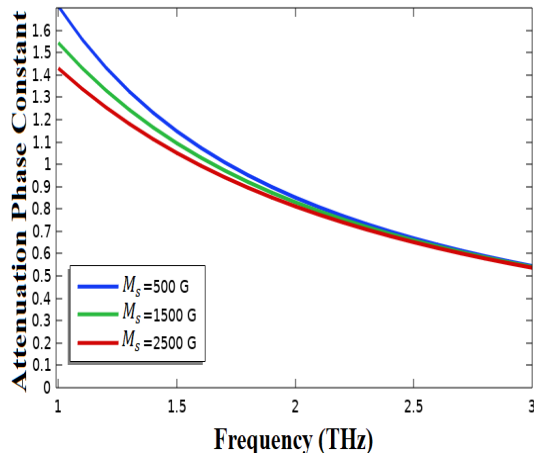


Fig. 11. Influence of saturation magnetization on attenuation phase for ferrite-graphene-ferrite waveguide.

The graphical pictures in fig.10. evidence the fact that increasing saturation magnetization the normalized phase constant is increasing and propagation of waves are moving toward low frequency region. On the other side the same values are taken for the attenuation, and it has been observed that increasing saturation magnetization has a direct impact on the attenuation phase constant and subsequently on propagation losses. As saturation magnetization increases, the alignment of magnetic domains improves, leading to a reduction in losses during wave propagation. This tunability of magnetic material is the best application for designing radar antenna and passive components such as isolators, phase shifters and circulators.

Figure 12 describes the effect of multilayers of graphene on the normalized phase constant  $Re\left(\frac{\beta}{k_0}\right)$  verses angular frequency. As the number of graphene layers increases the normalized phase for the curves also increases and shifts toward higher frequency region. By making an increment in number of graphene layers the electromagnetic surface propagation also varies and the curves are shifted towards low frequency region as reported in [28]. It is clear from the plot that as the number of graphene layers increases the bandgap also increases. Figure 13 describes the influence of number of graphene layers on the attenuation phase constant  $Im\left(\frac{\beta}{k_0}\right)$  verses angular frequency. The numbers of graphene layers considered are  $N = 1$ ,  $N = 2$ , and  $N = 3$  represented by the blue, green, and red color respectively.

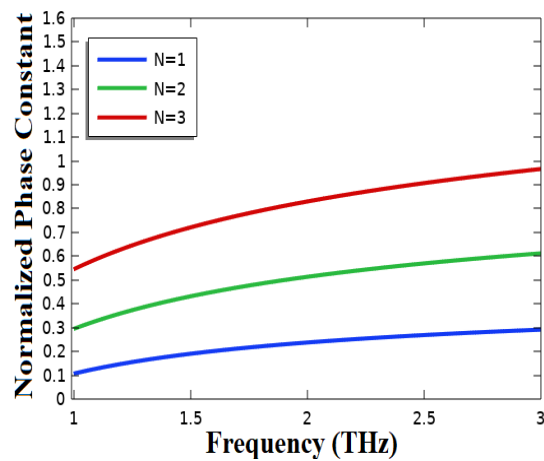


Fig. 12. Influence of graphene layers on the normalized phase constant for ferrite-graphene-ferrite waveguide structure.

The plot depicts that the propagation losses are larger at single layer and increment in layers reduces the propagation losses. Figures 14 and 15 represent the distribution of magnetic and electric field, to understand the mechanism of proposed ferrite-graphene-ferrite waveguide structure at THz frequency. The surface plot demonstrates that the surface plasmons polaritons are travelling in the graphene medium and the maximum electric field is localized in the graphene plane.

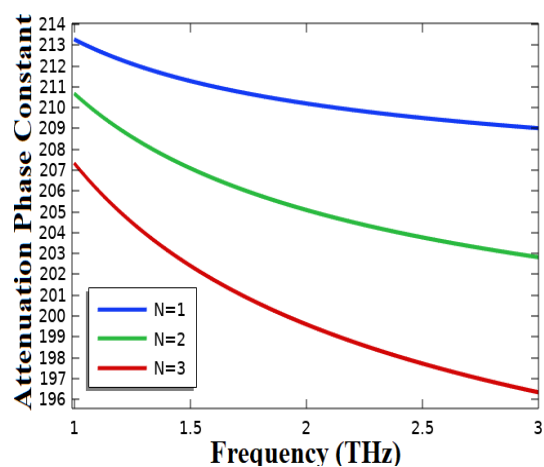


Fig. 13. Influence of graphene layers on the attenuation phase constant for ferrite-graphene-ferrite waveguide structure..

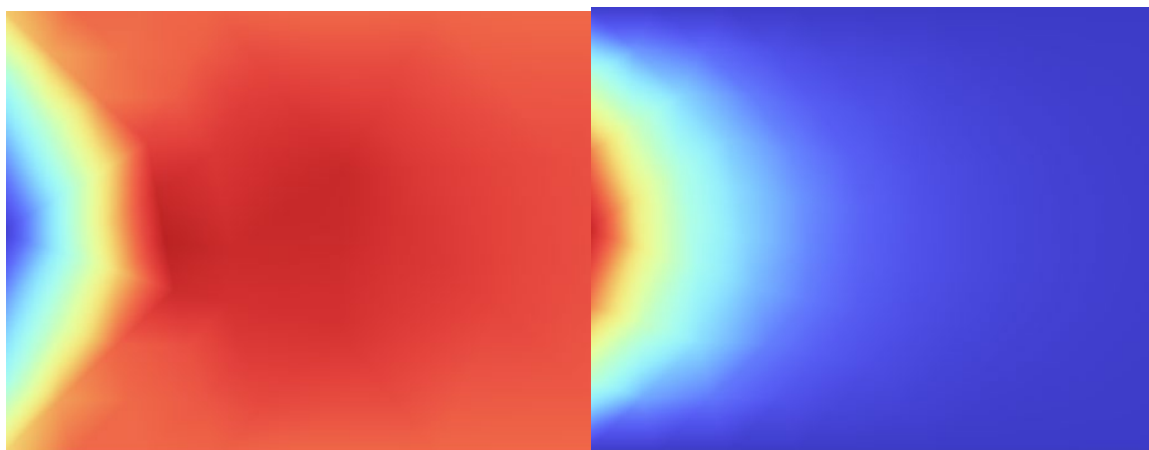


Fig. 14. Distribution of magnetic field in THz. Fig. 15. Distribution of electric field in THz.

#### 4. Conclusion

The theoretical simulation has been done for the investigation of propagation of EMSWs in graphene surrounded by ferrite film. Comsol Multiphysics software is used for simulation purposes. The impact of various parameters such as chemical potential, relaxation time, number of graphene layers, dielectric constant of ferrite, magnetic field, and saturation magnetization on the normalized phase  $Re\left(\frac{\beta}{k_o}\right)$  and attenuation phase constant  $Im\left(\frac{\beta}{k_o}\right)$  verse angular frequency in terahertz frequency are analyzed. The graphical pictures depict that as the relaxation time and chemical potential, number of graphene layers, magnetic field, dielectric constant of ferrite film and saturation magnetization increases, the normalized phase tends to increase and propagation of EMSWs shifts towards high frequency region. The propagation losses are minimized by increasing above parameters. The presented work has the potential to open new avenues to fabricate nanophotonic chips.

#### Acknowledgements

The authors extend their appreciation to the Deputyship for Research & Innovation, Ministry of Education in Saudi Arabia for funding this research work through the project number (IF2/PSAU/2022/01/23149).

#### References

- [1] Datsko, V.N., A.A. Kopylov, On surface electromagnetic waves. 2008, UFN; <https://doi.org/10.3367/UFNr.0178.200801f.0109>
- [2] Heydari, M.B., Optik, 2022. 254: p. 168651; <https://doi.org/10.1016/j.ijleo.2022.168651>
- [3] Heydari, M.B., M.H. Vadjed Samiei, Optical and Quantum Electronics, 2020. 52(9): p. 406; <https://doi.org/10.1007/s11082-020-02525-z>
- [4] Zhang, J., L. Zhang, W. Xu, Journal of Physics D: Applied Physics, 2012. 45(11): p. 113001; <https://doi.org/10.1088/0022-3727/45/11/113001>
- [5] Kim, J.T., C.-G. Choi, Optics express, 2012. 20(4): p. 3556-3562; <https://doi.org/10.1364/OE.20.003556>
- [6] de Oliveira, R.E., C.J. de Matos, Scientific Reports, 2015. 5(1): p. 16949; <https://doi.org/10.1038/srep16949>
- [7] Kim, J.T., K.H. Chung, C.-G. Choi, Optics Express, 2013. 21(13): p. 15280-15286;

<https://doi.org/10.1364/OE.21.015280>

[8] Wu, Y., et al., IEEE Journal of selected topics in Quantum Electronics, 2013. 20(1): p. 49-54; <https://doi.org/10.1109/JSTQE.2013.2263117>

[9] Teng, D., et al., Applied Physics B, 2020. 126: p. 1-9; <https://doi.org/10.1007/s00340-020-07525-1>

[10] Teng, D., et al., Optical Materials, 2022. 128: p. 112436; <https://doi.org/10.1016/j.optmat.2022.112436>

[11] Mohammadi, M., F.H. Kashani, J. Ghalibafan, Journal of Magnetism and Magnetic Materials, 2019. 491: p. 165551; <https://doi.org/10.1016/j.jmmm.2019.165551>

[12] Ghalibafan, J., N. Komjani, B. Rejaei, IEEE transactions on magnetics, 2013. 49(8): p. 4780-4784; <https://doi.org/10.1109/TMAG.2013.2245336>

[13] Zhang, G., et al., Journal of Magnetism and Magnetic Materials, 2017. 436: p. 57-60; <https://doi.org/10.1016/j.jmmm.2017.04.027>

[14] Hwang, K.C., H.J. Eom, IEEE Microwave and wireless components letters, 2005. 15(5): p. 345-347; <https://doi.org/10.1109/LMWC.2005.847651>

[15] Hosseininejad, S.E., N. Komjani, IEEE Transactions on Antennas and Propagation, 2016. 64(9): p. 3787-3793; <https://doi.org/10.1109/TAP.2016.2583538>

[16] Shkerdin, G., et al., IET Microwaves, Antennas & Propagation, 2016. 10(6): p. 692-699; <https://doi.org/10.1049/iet-map.2015.0365>

[17] Zhu, B., et al., Optics express, 2013. 21(14): p. 17089-17096; <https://doi.org/10.1364/OE.21.017089>

[18] Seewald, C.K., J.R. Bray, IEEE Transactions on Microwave Theory and Techniques, 2010. 58(6): p. 1493-1501; <https://doi.org/10.1109/TMTT.2010.2047919>

[19] Dadoenkova, Y.S., et al., Annalen der Physik, 2017. 529(5): p. 1700037; <https://doi.org/10.1002/andp.201700037>

[20] Bao, J., et al., Journal of Micromanufacturing, 2020. 3(1): p. 20-27; <https://doi.org/10.1177/2516598419896130>

[21] Heydari, M.B.; M.H.V. Samiei, Plasmonic graphene waveguides: A literature review. arXiv preprint arXiv:1809.09937, 2018.

[22] Gric, T., E. Rafailov, Optik, 2022. 254: p. 168678; <https://doi.org/10.1016/j.ijleo.2022.168678>

[23] Gric, T., O. Hess, Applied Sciences, 2018. 8(8): p. 1222; <https://doi.org/10.3390/app8081222>

[24] Toqeer, I., et al., Optik, 2019. 186: p. 28-33; <https://doi.org/10.1016/j.ijleo.2019.04.013>

[25] Ali, R., B. Zamir, H. Shah, Results in physics, 2018. 8: p. 243-248; <https://doi.org/10.1016/j.rinp.2017.11.037>

[26] Hirani, R.R., et al., AEU-International Journal of Electronics and Communications, 2018. 83: p. 123-130; <https://doi.org/10.1016/j.aeue.2017.08.019>

[27] Ioannidis, T., T. Gric, E. Rafailov, Optical and quantum electronics, 2020. 52: p. 1-12; <https://doi.org/10.1007/s11082-019-2128-x>

[28] Gric, T., O. Hess, Optics express, 2017. 25(10): p. 11466-11476; <https://doi.org/10.1364/OE.25.011466>

[29] Teng, D., et al., Results in Physics, 2020. 17: p. 103169; <https://doi.org/10.1016/j.rinp.2020.103169>